Inverse Design A 3D Printed Four-Port Power Splitter Leveraging Gradient Optimization and Adjoint Method

Saeed Zolfaghary pour
Electrical and Computer
Engineering Department,
FAMU-FSU College of
engineering
Tallahasse, United States
Saeed1.zolfagharypou@famu.edu

Hanxiang Zhang
Electrical and Computer
Engineering Department,
FAMU-FSU College of
engineering
Tallahasse, United States
hz21c@fsu.edu

Powei Liu

Electrical and Computer
Engineering Department,
FAMU-FSU College of
engineering
Tallahasse, United States
pl21h@fsu.edu

Hao Yan

Electrical and Computer
Engineering Department,
FAMU-FSU College of
engineering
Tallahasse, United States
hy23n@fsu.edu

Jonathan Casamayor

Electrical and Computer Engineering

Department,

FAMU-FSU College of engineering

Tallahasse, United States

jc02@fsu.edu

Mitch Plaisir

Electrical and Computer Engineering
Department,

FAMU-FSU College of engineering
Tallahasse, United States
mep18m@fsu.edu

Bayaner Arigong
Electrical and Computer Engineering
Department
FAMU-FSU College of Engineering
Tallahasse, United States
barigong@eng.famu.fsu.edu

Abstract— In this paper, a novel inverse design approach is presented to design and 3D print multiport RF/Microwave devices. The proposed inverse design method integrates the gradient optimization with the adjoint method to calculate and average multiple independent objective functions at each iteration for constructing a desirable multiport S-parameter matrix. To validate the proposed design concept, a prototype is fabricated using 3D printing technology. The simulation and measurement results agree well with each other to demonstrate proposed inverse design approach. This marks the first instance of employing the inverse design method to design a multiport microwave device, subsequently realized through 3D printing technology to enable tailored characteristics and versatility.

Keywords— Inverse design, directional coupler, power splitter, 3D printing, adjoint method, gradient optimization

I. INTRODUCTION

Power splitters are passive components in RF/Microwave applications, which divide the input power into several output ports with different power division ratios. Most of the current power splitters or combiners [1]-[3] as Wilkinson, branch line hybrid, and rat-race are designed from forward method with known topologies, and multiport devices exceeding number of ports more than four are designed by cascading those known devices. However, in practical design, there is a demand for power splitter or combiner designs with an arbitrary number of ports and configurations that can fit into the system needs. Developing these types of power splitters/combiners is challenging using conventional forward design methods. Therefore, inverse design is one possible method to overcome this challenge, which can identify the optimum circuit structure based on given input and output signals and power ratio constraint. Inverse design of the electromagnetic structures is

invented first for two-dimensional nanophotonic device designs [4]–[7], and it is then investigated to design 3D structures for the optical domain by developing different computational optimization techniques. Leveraging image processing technique [8], gradient optimization offers unparalleled design freedom to update material distribution locally inside the design space domain so that it can be widely applied to design multifunctional metasurface [9] and photonic crystal electromagnetic devices [10] instead of implementing conventional design method which is based on circuit theory [11]-[12] or optimization [13]. Several microwave passive circuits are currently designed from inverse design approach [14]–[16]. For example, in [16], a broadband radio frequency translator from a printed circuit board to a waveguide or horn antenna is designed from gradient optimization to achieve excellent shielding, low loss, and high power handling properties.

In this paper, a four-port power splitter operating at 10 GHz is designed from inverse design approach using gradient optimization and adjoint sensitivity analysis method. Multiple objective functions, one for each of the four ports, are applied to distinct the functionality for each port excitation. The gradients of multiple objective functions, with respect to all design parameters, are computed using the adjoint method. To realize proposed power divider design, a 3D printing technology is employed, and the geometric constraint method is applied to strategically align the design with the specifications inherent to the 3D printer. This deliberate alignment ensures a harmonious integration of the proposed design within the parameters of the chosen fabrication technology.

II. THEORY AND FORMULATION

A. Optimization principle and djoint method

The primary objective of inverse design is to determine a set of design variables denoted as ρ , which maximize an objective function $\varphi = \varphi(E, E^*, \rho)$. Here, φ is a complex function of its arguments, and E is a complex value vector in a linear system. In this work, E denotes the electric field solution to linear Maxwell equations. Noted that the design variables are considered real value, and ρ is a function of material density over the design region. In a design region comprising a dielectric (with relative permittivity of $\varepsilon_{\rm m}$) and free space, the description of ρ can be determined at the location of r as follow:

$$\rho(r) = \frac{\varepsilon_r(r) - 1}{\varepsilon_m - 1} \tag{1}$$

Here, $\varepsilon_{\rm r}(r)$ is a function with maximum value of $\varepsilon_{\rm m}$ and minimum value of 1. Consequently, the value of $\rho(r_0)$ at the location r_0 varies from 0 in the case of free space to 1 in the case of the dielectric.

To maximize the objective function with respect to the design variables, it is crucial to compute the sensitivity with respect to each element. The sensitivity is expressed as:

$$\frac{d\varphi}{d\rho} = \frac{d\varphi}{d\rho} + \frac{\partial\varphi}{\partial E} + \frac{\partial\varphi}{\partial E^*} \frac{\partial E^*}{\partial\rho}$$
 (2)

The equation (2) can be further simplified based on [7] to achieve:

$$\frac{d\varphi}{d\rho} = \frac{d\varphi}{d\rho} + 2\operatorname{Re}\left\{E_{adj}^{T}\frac{\partial f}{\partial\rho}\right\} \tag{3}$$

Where E_{adj} is the complex-valued adjoint electric field, and f represents the linear Maxwell's equations that E is its solution $(f(E, E^*, \rho) = 0)$.

To inverse design multiport device, multiple objective functions are formulated for designing proposed four port power splitter, which have different functionality when each different port is excited. For any reciprocal, lossless, and matched four-port network referred to as a directional coupler [3], the scattering parameters of this four-port directional coupler is described as follow:

$$S = \begin{bmatrix} 0 & S_{12} & 0 & S_{14} \\ S_{12} & 0 & S_{23} & 0 \\ 0 & S_{23} & 0 & S_{34} \\ S_{14} & 0 & S_{34} & 0 \end{bmatrix}$$

$$(4)$$

From the S matrix, the constrained optimization problems are: 1) no reflection for each port excitation; 2) the incident power is guided to two output ports with desired power ratio; 3) the power loss in this device is zero. To achieve these conditions, in this design, four different optimizations are conducted, and the new optimization objective function is formulated as a set of sub-objective functions:

$$\varphi_{new} = \sum_{n=1}^{4} \frac{\varphi_n}{4} \tag{5}$$

$$\varphi_n = \prod_{m=1(m \neq n, i)}^{4} \left[\left| E_m^2 \right| \right] - \left| E_i^2 \right| \tag{6}$$

 $E_{\rm m}$ represents the electric field intensity at $m^{\rm th}$ port, where power is evenly split among the two outputs and $E_{\rm i}$ represents the electric field intensity at the isolated port. The sensitivity of the new objective function can be calculated by averaging the sensitivity of all sub-objective functions:

B. S-parameters analysis

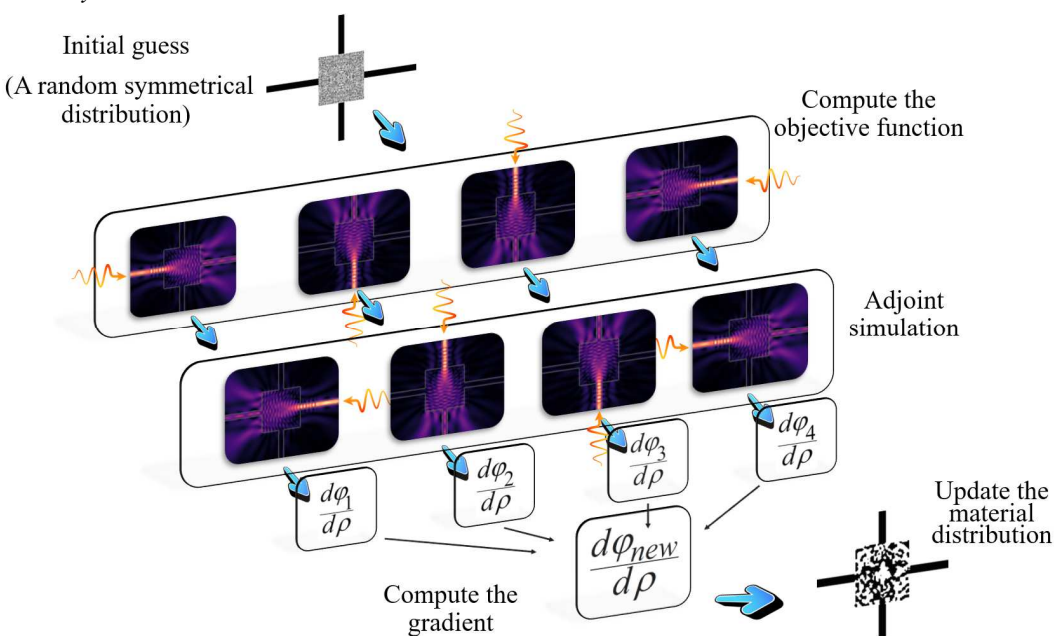


Fig. 1. The process of optimizing the design of a four-port power splitter involves several key steps. It commences with the establishment of an initial estimation for the distribution within the design region. Subsequently, a series of forward and adjoint simulations are meticulously executed during each iteration to discern and refine the optimal gradient.

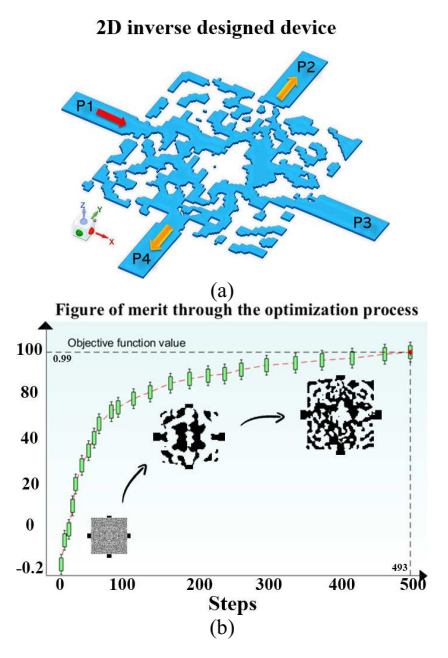


Fig. 2. (a) Bird's-eye view of design region and the optimized 4 port power splitter. (b) Objective function value verse iteration number.

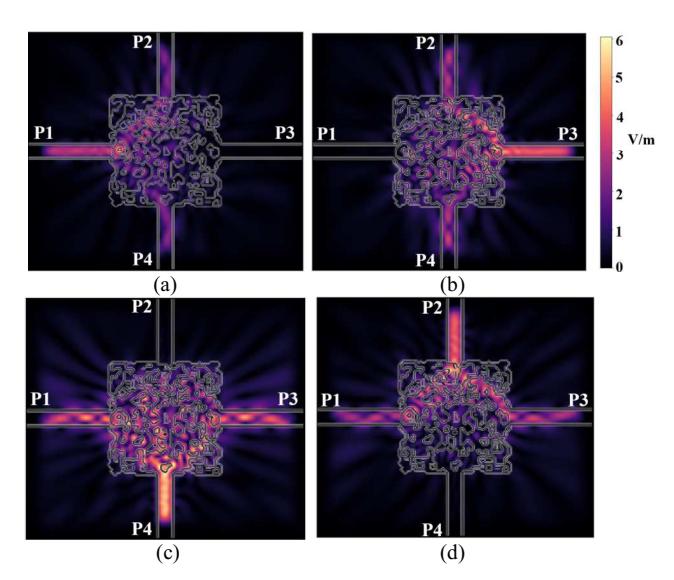


Fig. 3. The electric field distribution of the 2D FEM when port (a) P1 (b) P3 (c) P4 (d) P2 is excited as input.

$$\frac{d\varphi_{\text{new}}}{d\rho} = \sum \frac{d\varphi_n}{d\rho} \tag{7}$$

$$\frac{d\varphi_n}{d\rho} = \frac{d\varphi_n}{d\rho} + 2\operatorname{Re}\left\{E_{adj_n}^T \frac{\partial f}{\partial \rho}\right\}$$
(8)

where E_{adjn} is the electric field of the adjoint simulation while φ_n is computing. Equation (6) is valued for a symmetric power splitter with equal power ratio at the two outputs. By altering this constraint and modifying equation (5), one can achieve a custom four port with any arbitrary power ratio.

III. DESIGN AND SIMULATION

A four-port device working at 10 GHz is optimized in a

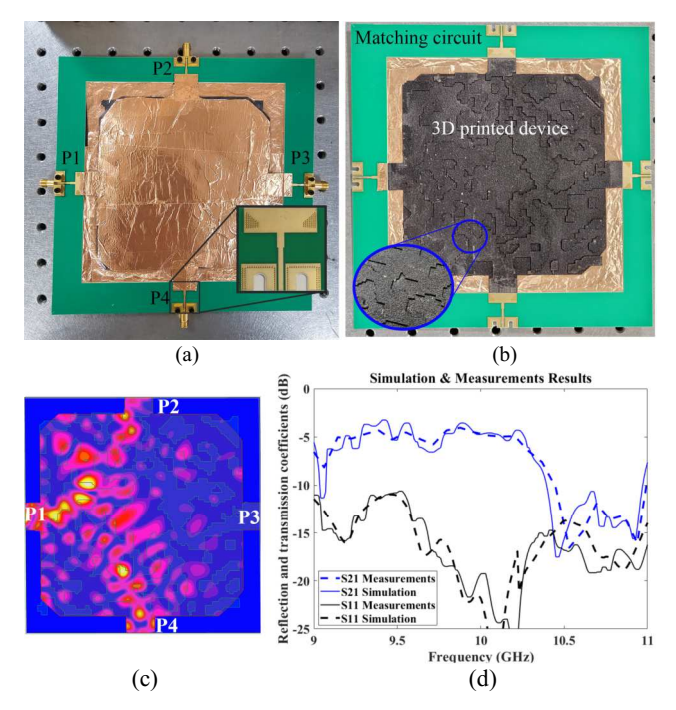


Fig. 4. The proposed fabricated structure for working at 10 GHz (a) with the top copper layer, (b) without the top layer (c) The electric field intensity distribution when the port P1 is excited. (d) The measured and simulated S-parameters for input (reflection coefficient) and the outputs (transmission coefficient).

12cm \times 12cm design region with relative permittivity of ε_r = 3.6 (Polyamide Nylon 12). Polyamide Nylon is chosen because it is a commercially available raw material for 3D printing. The constraints of avoiding small overall dimensions and maintaining a minimum feature size to achieve a manufacturable final structure are retained as outlined in the reference [17]. The minimum radius of curvature for the minimum feature size is set to 4mm, and the optimization is carried out in a 2D space where a normalized polarized wave is excited on the 2D plane to reduce the computational cost at each iteration. The optimization procedure is illustrated in Fig. 1 beginning with an initial guess of a symmetrical random distribution of dielectric material across the design region. Here, the initial symmetrical random distribution helps the optimization algorithm to find a symmetrical solution for our problem. The forward and adjoint simulations for each different port excitation are carried out to find the optimum gradient for the next iterations.

The optimized structure is shown in Fig. 2 (a). The figure of merit in equation (5) verse iteration number is shown in Fig. 2 (b). The value of objective function is starting from 0 for 0% efficiency to 1 for 100% efficiency when two outputs are receiving the maximum equal power from input port. Fig. 3 shows the electric field distribution for each port excitation. The simulation and optimization are carried out by using finite element method (FEM). The optimization process seeks to maximize equation (5) with the gradient of each iteration computed through equation (7).

Since the polarization of the electric field is set orthogonal to the inverse design region, two metal sheets are applied at the top and bottom of the dielectric distribution, respectively. Bottom metal sheet acts as a ground, and the top serves as a trace which keeps a slight separation between bottom metal maintaining orthogonal electric field polarization as shown in Fig. 4(a). Fig. 4(b) shows the 3D printed structure without the top metallic layer. The thickness of the inverse-designed dielectric and substrate of waveguides are set to 510 µm to maintain a desired profile for electric field distribution. The tapering technique is employed to reduce unwanted radiation from square edges, thereby enhancing the overall performance of the final structure. To measure the proposed 3D printed fourport device, a coaxial-microstrip-waveguide transition structure is designed to connect the four port to network analyzer. As shown in Fig. 4 (a), these matching circuit is designed using PCB fabrication technology, and the substrate is Rogers 4350B with dielectric constant of 3.48. The dielectric, designed using the inverse approach, is manufactured using 3D printing and is composed of Nylon as shown in Fig. 4(b). The prototype is fabricated using 3D printing multi jet fusion technology that is suitable for manufacturing 2.5 devices, and it enables rapid prototyping. The distribution of the electric field intensity for this device is illustrated in Fig. 4(c), where the power is equally divided into two ports (P_2 and P_3) for port P_1 excitation. The simulation is carried out using Ansys HFSS simulation software. The inverse designed medium guides the field to propagate through the outputs with minimum leakage to the isolation port P_3 , even though the isolation port is place directly at the front of the input. The reflection coefficient at port 1 and the transmission coefficient at port 2 are shown in Fig. 4(d), where the reflection coefficient is better than 20 dB. The transmission coefficient is around -4.5 dB at design frequency 10 GHz, and the operating bandwidth is more than 500 MHz. The presence of the background 3D printed substrate causes dielectric loss for transmission, which can be mitigated by decreasing the thickness of the background as much as possible with high quality printable dielectric material.

IV. CONCLUSION

This paper introduces a prototype for the inverse design of a four-port power splitter for microwave regime leveraging 3D printing technology. The proposed inverse design approach combines the gradient optimization method and the adjoint analysis method to determine optimal gradients at each iteration for multiple objective functions, where multiple independent optimizations are averaged at each iteration to create the desirable S-parameter matrix. To prove our design concept, designing multiport microwave device using inverse design, a prototype is fabricated using 3D printing technology, and the simulation and measurement results align well with each other to demonstrate the proposed idea. This is first time a microwave

device is designed using inverse design method and implemented using 3D printer, which provides an efficacy and reliability approach for designing power splitters with customizable characteristics and performances.

REFERENCES

- [1] O. A. Ivanov, V. A. Isaev, M. A. Lobaev, A. L. Vikharev, and J. L. Hirshfield, "High power microwave switch employing electron beam triggering with application to active rf pulse compressors," *Phys. Rev. ST Accel. Beams*, vol. 14, no. 6, p. 061301, Jun. 2011.
- [2] H. Xu, D. Dai, and Y. Shi, "Ultra-broadband on-chip multimode power splitter with an arbitrary splitting ratio," OSA Continuum, OSAC, vol. 3, no. 5, pp. 1212–1221, May 2020.
- [3] D. M. Pozar, Microwave Engineering. John Wiley & Sons, 2011.
- [4] S. Molesky, Z. Lin, A. Y. Piggott, W. Jin, J. Vucković, and A. W. Rodriguez, "Inverse design in nanophotonics," *Nature Photon*, vol. 12, no. 11, Art. no. 11, Nov. 2018.
- [5] K. Yao, R. Unni, and Y. Zheng, "Intelligent nanophotonics: merging photonics and artificial intelligence at the nanoscale," *Nanophotonics*, vol. 8, no. 3, pp. 339–366, Mar. 2019.
- [6] M. D. Huntington, L. J. Lauhon, and T. W. Odom, "Subwavelength Lattice Optics by Evolutionary Design," *Nano Lett.*, vol. 14, no. 12, pp. 7195–7200, Dec. 2014.
- [7] T. W. Hughes, M. Minkov, I. A. D. Williamson, and S. Fan, "Adjoint Method and Inverse Design for Nonlinear Nanophotonic Devices," ACS Photonics, vol. 5, no. 12, pp. 4781–4787, Dec. 2018.
- [8] R. E. Christiansen and O. Sigmund, "Inverse design in photonics by topology optimization: tutorial," *J. Opt. Soc. Am. B, JOSAB*, vol. 38, no. 2, pp. 496–509, Feb. 2021.
- [9] Z. Lin, V. Liu, R. Pestourie, and S. G. Johnson, "Topology optimization of freeform large-area metasurfaces," *Opt. Express, OE*, vol. 27, no. 11, pp. 15765–15775, May 2019.
- [10] J. S. Jensen and O. Sigmund, "Systematic design of photonic crystal structures using topology optimization: Low-loss waveguide bends," *Appl. Phys. Lett.*, vol. 84, no. 12, pp. 2022–2024, Mar. 2004.
- [11] S. Zolfaghary pour, E. Chegini, and M. Mighani, "Design of wideband metamaterial absorber using circuit theory for X band applications" *IET Microwaves, Antennas & Propagation*, vol. 17, no. 4, pp. 292-300, Mar. 2023.
- [12] S. Zolfaghary pour, A. Khavasi, and B. Rejaei, "Design and Fabrication of a Polarization-Independent Millimeter-Wave Absorber Using Circuit Theory and 3D Printing," *Journal of Electronic Materials*, vol. 53, no. 1, pp. 525-534, Jan. 2024.
- [13] S. Zolfaghary pour, and K. Arik, "Ultra-broadband polarization-independent perfect absorber based on phase change material (Ge 2 Sb 2 Te 5 or GST) for the visible and infrared regions," *Optical and Quantum Electronics*, vol. 55, no. 2, pp. 141, Feb. 2024.
- [14] S. Ayhan, S. Scherr, P. Pahl, S. Wälde, M. Pauli, and T. Zwick, "Radar-Based High-Accuracy Angle Measurement Sensor Operating in the K-Band," *IEEE Sensors Journal*, vol. 15, no. 2, pp. 937–945, Feb. 2015.
- [15] B. Scheiner, F. Lurz, F. Michler, S. Linz, R. Weigel, and A. Koelpin, "Six-Port Based Multitone and Low-Power Radar System for Waveguide Measurements in Smart Factories," in 2018 48th European Microwave Conference (EuMC), Sep. 2018, pp. 1065–1068.
- [16] E. Hassan et al., "Multilayer Topology Optimization of Wideband SIW-to-Waveguide Transitions," *IEEE Transactions on Microwave Theory and Techniques*, vol. 68, no. 4, pp. 1326–1339, Apr. 2020.
- [17] Y. Zhang et al., "A compact and low loss Y-junction for submicron silicon waveguide," Opt. Express, OE, vol. 21, no. 1, pp. 1310–1316, Jan. 2013.